

Research Article

Xichao Xia*, Guina Liang, Xinhua Zheng, Fuan Wang, Junfeng Zhang, Shipeng Xue, Chuanxiu Hua, Guoying Song, Xianguang Bai and Lianghong Guo*



Characterization of calmodulin in the clam *Anodonta woodiana*: differential expressions in response to environmental Ca^{2+} and Cd^{2+}

Tatlı su midyesi *Anodonta woodiana* için kalmadulin tanımlaması: Çevresel Ca^{2+} ve Cd^{2+} yanıtta diferansiyel ekspresyon

<https://doi.org/10.1515/tjb-2017-0168>

Received June 24, 2017; accepted October 3, 2017; previously published online January 5, 2018

Abstract

Aims: To explore effect of Ca^{2+} and Cd^{2+} on the calmodulin (CaM), one complete cDNA sequence (AwCaM1) was cloned and characterized from the freshwater mussel *Anodonta woodiana* and its expressions were analyzed.

Materials and methods: The AwCaM1 was cloned from the *A. woodiana* using the rapid amplification of cDNA ends methods and its expression was determined by real-time PCR.

Results: In the hepatopancreas, AwCaM1 expression was up-regulated with a time and dose dependent pattern in the Ca^{2+} treated groups (0.01, 0.02, 0.04 and 0.08 mg/L) during experiment observed, and increased more than

56.15% ($p < 0.05$) compared with that of control group. AwCaM1 mRNA level increased more 65.04% ($p < 0.05$) in the Cd^{2+} treated groups (8 and 16 mg/L). In the gill, AwCaM1 expression increased more than 79.41% ($p < 0.05$) compared with that of control group in all the Ca^{2+} treated groups, and more than 88.23% ($p < 0.05$) in all the Cd^{2+} treated groups.

Conclusion: These results indicated that up-regulations of AwCaM1 expression in bivalve *A. woodiana* are associated with Ca^{2+} absorb and environmental adaption derived from Ca^{2+} and Cd^{2+} treatment.

Keywords: *Anodonta woodiana*; AwCaM1; Up-regulations; Ca^{2+} ; Cd^{2+} .

Özet

Amaçlar: Ca^{2+} ve Cd^{2+} 'nin kalmadulin (CaM) üzerine etkisini araştırmak için tatlı su midyesi *Anodonta woodiana* 'dan tam bir cDNA dizisi (AwCaM1) klonlandı, karakterize edildi ve gen ifadeleri analiz edildi.

Materyal ve Metot: AwCaM1, *A. woodiana* 'dan cDNA uçlarının hızlı amplifikasyonu yöntemi kullanılarak klonlandı ve gen ifadesi gerçek zamanlı PCR ile belirlendi.

Bulgular: Hepatopankreasta AwCaM1 ekspresyonu, zamana ve doza bağımlı olarak Ca^{2+} ile muamele edilen gruplarda (0.01, 0.02, 0.04 ve 0.08 mg/L) upregüle edildi ve kontrol grubuna kıyasla %56.15'den ($p < 0.05$) fazla arttı. AwCaM1 mRNA seviyesi, Cd^{2+} ile muamele edilen gruplarda (8 ve 16 mg/L) % 65.04'den ($p < 0.05$) fazla arttı. Solungaçta AwCaM1 ekspresyonu, tüm Ca^{2+} ile muamele edilen gruplarda kontrol grubuna kıyasla %79.41'den

*Corresponding authors: Xichao Xia, Medical College of Pingdingshan University, Pingdingshan, 467000 Henan Province, China, e-mail: xiaxichao8336@163.com.
http://orcid.org/0000-0001-7836-8110; and State Key Laboratory of Environmental Chemistry and Eco-toxicology, Research Center for Eco-environmental Sciences, Chinese Academy of Sciences, Beijing 100085, China; and Lianghong Guo, State Key Laboratory of Environmental Chemistry and Eco-toxicology, Research Center for Eco-environmental Sciences, Chinese Academy of Sciences, Beijing 100085, China, e-mail: lhguo@rcees.ac.cn

Guina Liang, Shipeng Xue and Chuanxiu Hua: Basic Medicine College of Nanyang Medical University, Nanyang, 473041 Henan Province, China

Xinhua Zheng, Fuan Wang, Junfeng Zhang, Guoying Song and Xianguang Bai: Medical College of Pingdingshan University, Pingdingshan, 467000 Henan Province, China

($p < 0.05$) ve tüm Cd^{+2} ile muamele edilen gruplarda %88.23'den ($p < 0.05$) fazla arttı.

Sonuç: Bu sonuçlar, *A. woodiana*'da AwCaM1 ekspresyonunun up-regülasyonlarının, Ca^{+2} ve Cd^{+2} muamelesinden kaynaklanan Ca^{+2} emilimi ve çevre adaptasyonu ile ilişkili olduğunu gösterdi.

Anahtar Kelimeler: *Anodonta woodiana*; AwCaM1; Up-regülasyon; Ca^{2+} ; Cd^{2+} .

Introduction

An array of test organisms, including amphipods, polychaetes, mollusks, crustaceans and fish have been recommended for use in sediment toxicity tests [1]. While this array of test organisms covers a diverse group of fauna, many of them may not be indigenous to all geographic locations [2]. As a group of sedimentary organism, the bivalve filter feeds on suspended particulates and phytoplankton [2]. Their habitat is vulnerable to pollution from urban and industrial development. In addition, adults do not migrate, repopulation of over-fished hard-clam beds depends on the transport of larvae from other areas and several years are required for growth, maturation and reproduction [3]. Using water concentrations associated with response of organism as an indicator of sensitivity, bivalves appear more sensitive to environmental pollution than do other invertebrates [4]. Freshwater clams, *Anodonta woodiana* are widely distributed in the world and functions as a main criteria required for a bio-indicator organism. Earlier studies have revealed the ability of *A. woodiana* to accumulate trace elements and pesticides, as well as its potential to detect genotoxicity [5]. In addition, these mussels have important ecosystem functions such as particle filtration and processing, nutrient release and sediment mixing [6]. Unfortunately, metal pollution has resulted in a tremendous threat on their population that can profoundly affect food chain and aquatic ecosystem. Cadmium (Cd), a non-essential metal element required for many of living organisms, can easily enter the environment as a pollutant from many anthropogenic activities [7]. Now, Cd is one of seven most common released heavy metals for the environment (Cd, Cr, Cu, Hg, Ni, Pb and Zn) and its existence causes a serious threat on many invertebrates in aquatic environment, such as crustacean, gastropod mollusks and bivalve [8].

Great evidences have demonstrated intracellular Ca^{2+} mediates a large number of cellular responses with the high affinity and specificity required for a regulatory second messenger [9]. Calmodulin (CaM), a Ca^{2+} -binding

protein, is a ubiquitous, highly conserved, eukaryotic protein that binds and regulates a number of diverse target proteins involved in programmed cell death, autophagy, muscle contraction, inflammation and the immune response [9]. When bound to Ca^{2+} , CaM is able to further bind to CaM-binding proteins (CaMBPs) and directly regulate activities of target proteins [9]. Through the action of these CaMBPs, CaM is involved into a great variety of cellular processes, such as protein translation, protein phosphorylation, cell cycle and cyclic nucleotide metabolism [10]. Notably, several lines of in vitro evidence indicate Cd^{2+} , which has a similar ionic radius to Ca^{2+} , can also bind CaM influencing these downstream effector proteins [11]. A recent in vitro study using osteoblasts derived from rat fetal, demonstrates that Cd^{2+} treatment significantly increases intracellular Ca^{2+} , leads to CaM activation and ultimately apoptotic death of cells [12]. Other studies specifically implicate the CAMKII pathway as being activated by Cd^{2+} exposure resulting in apoptosis in cultured mesangial and neuronal cells [13].

Studies on Cd^{2+} -induced toxicological effects have been underdone in the vertebrate, but the mechanisms underlying of observed responses are needed to further elucidate in the invertebrate. Take into consideration of great interest to investigate the effect of metals on *A. woodiana*, in the current study, one complete cDNA sequence and two premature termination codon mutations of CaM have been cloned and respectively named AwCaM1, AwCaM2 and AwCaM3. In addition, spatio-temporal expressions of AwCaM1 derived from Ca^{2+} and Cd^{2+} exposure were determined by quantitative real-time PCR. The present study should be helpful to elucidate the regulatory network of AwCaM1 derived from Ca^{2+} and Cd^{2+} treatment. Meanwhile, it also contribute to government paid attention to heavy metals diffusion and take measures to mitigate extensive negative impacts on freshwater organisms and conserve aquatic organism biodiversity.

Materials and methods

Ethics statement

All handling methods of clams were conducted in accordance with the guidelines on the care and use of animals for scientific purposes set up by the Institutional Animal Care and Use Committee of Pingdingshan Medicine College, Pingdingshan, China.

Materials

Approximately 1-year-old of clams *A. woodiana* (shell length, 6.5 ± 0.5 cm) were obtained from the Baihe River of Nanyang, Henan Province, China. Prior to experiment, animals were maintained in a recirculation system containing filtered freshwater at 24°C for 2 weeks in laboratory. The experiment was conducted in rectangular plastic boxes ($40\text{ cm} \times 25\text{ cm}$; 10 cm height). Clams were cultured in 10 L artificial pond water containing 48 mg NaHCO_3 , 33 mg $\text{CaCl}_2 \cdot 2\text{H}_2\text{O}$, 60 mg $\text{MgSO}_4 \cdot 7\text{H}_2\text{O}$ and 0.5 mg KCl per 1 L deionized water, with a pH of 7.0 [14]. In order to determine the tissue distribution of AwCaM1, five clams derived from same tank were dissected, and several of tissues including foot, gill, hepatopancreas, adductor muscle, heart, hemocytes and mantle were sampled prior to the treatment.

In a Ca and Cd concentration gradient experiment, 330 clams were randomly divided into 11 groups. Each group of 30 specimens was placed into three replicate tanks (10 clams per tank). One group of 30 was used as the control, and the other 10 groups were respectively treated with different concentrations of Ca (as CaCl_2 , 0.01, 0.02, 0.04, 0.08 and 0.16 mg/L) and Cd (as CdCl_2 , 1, 2, 4, 8 and 16 mg/L) [15, 16]. In the Ca^{2+} and Cd^{2+} incubation treatments, water was replaced with a fresh solution every day in order to assure both the water quality and a constant Ca^{2+} and Cd^{2+} content in the medium. Five individuals of each treatment group were randomly sampled at 0, 6, 12, 24, 48 and 72 h, and the hepatopancreas, gill and mantle were collected and stored at -80°C for quantitative real-time reverse transcriptase PCR (qRT-PCR).

Siphoning behavior

The siphoning rate was measured using a previously described method [17] with slight modifications and was based on depletion of neutral red dye particles from the water due to filtration by the clams. Immediately after Ca^{2+} and Cd^{2+} exposure, five clams *A. woodiana* from each Ca^{2+} and Cd^{2+} concentration group and control group were placed in 200 mL beakers that contained 100 mL of a neutral red solution and were allowed to siphon for 2 h. Just prior to placing the clams *A. woodiana* in the solution and just after the 2 h siphoning period, 1 mL aliquots of the water were removed from each beaker, and the neutral red concentration was determined by measuring the optical density at 530 nm using a spectrophotometer. Standard solutions of neutral red were used to generate a standard curve from which the dye concentrations in each test sample were calculated using the equation: where M is the volume of the

test solution, n is the number of clams used, t is the time in hours, C_0 is the initial concentration of the dye, C_t is the concentration of the dye at time t , and m is the filtration rate

$$m = \left[\frac{M}{nt} \right] \log \left(\frac{C_0}{C_t} \right)$$

Total RNA isolation and reverse transcription

Total RNA was extracted using TRIzol (Invitrogen Life Technologies, USA) according to the manufacturer's protocol. Quality of RNA was monitored by 1.2% agarose gel electrophoresis and those with complete rRNA bands were selected to produce cDNA. First-strand cDNA was synthesized using M-MLV First-Strand cDNA synthesis Kit (Takara, China) according to the manufacturer's instructions and used as the template for PCR reaction.

Cloning of AwCaM cDNA

CaM fragment was amplified using two degenerate primers CaM1 and CaM2 (Table 1) designed according to conserved domains of CaMs of other species including bivalve, gastropod, insect, crustacean and vertebrate. The PCR products were subcloned into the pMDT-19 (Takara, China), sequenced from both directions (Invitrogen Life

Table 1: Description of the primes used in this study.

Primer	Sequence (5'–3')
CaM1	CCATCNCTACNAAGNAANTGGG
CaM2	CTGCTNCACT NATANAGCNA TTTC
5' RACE Inner primer	CATGGCTACATGCTGACAGCCTA
5' RACE Outer primer	CGCGGATCCACAGCCTACTGATGATCAGTCGATG
AwCaM5-1	GTTCGGCCTCTGTTGGATTTTGCCC
AwCaM5-2	GTTCCATCCCCGTCCTTGTC
3' RACE Outer primer	TACCGTCGTTCCACTAGTGATTT
3' RACE Inner primer	CGCGGATCCTCCACTAGTGATTTCACTATAGG
AwCaM3-1	CTCGGGGAAAAGCTCAGACGAGG
AwCaM3-2	AGCAGATATTGACGGAGATGG
AwCaM-F	CAACAGAGGCCGAACCTCAG
AwCaM-R	CCTCGTCTGT GAGCTTTTCC C
β -F	CATCCCTTGCTCCTCCAATATG
β -R	CTGGAAGGTAGAGAGAGAAGCCAAG

CaM1 and CaM2 are degenerate primers and used to isolate partial cDNA of CaM. 5' RACE Outer primer, 5' RACE Inner primer, AwCaM5-1 and AwCaM5-2 are used to characterize the 5' RACE of the AwCaM in the nest PCR, 3' RACE Outer primer, 3' RACE Inner primer, AwCaM3-1 and AwCaM3-1 for 3' RACE. AwCaM-F and AwCaM-R as well as β -F and β -R are selected to isolate AwCaM1 and β -actin in real-time PCR, respectively.

Technologies, China) and identified CaM partial cDNA sequence. Highly stringent primers (Table 1) designed from the partial cDNA sequences were used to characterize the 5' and 3' region of the AwCaMs cDNA by rapid amplification of cDNA ends (RACE) approaches (Takara, China) according to the manufacturer's protocol. 5' RACE Outer primer and AwCaM5-1 (Table 1) were used for the first-round PCR of AwCaM 5' RACE, 3' RACE Outer primer and AwCaM3-1 (Table 1) for 3' RACE. Subsequently, 5' nested PCR was performed by the 5' first-round PCR product used as template, 5' RACE Inner primer included in the kit and AwCaM5-2, 3' nested PCR using 3' first-round PCR products, 3' RACE Inner primer and AwCaM3-2 (Table 1). The 5' RACE and 3' RACE nest PCR products were cloned and five clones were sequenced using the method described above.

Sequence and phylogenetic analysis

AwCaMs sequence were analyzed and compared using the BLAST program with a GenBank database search (www.ncbi.nlm.nih.gov/blast). The signal peptide was predicted by signal program (<http://www.cbs.dtu.dk/services/SignalP>). Prediction of protein domain was carried out with the Simple Modular Architecture Research Tool (<http://smart.embl-heidelberg.de/>). Multiple sequence alignments of AwCaMs gene were performed using the DANMEN analysis program. Prediction of three-dimensional (3D) structure was fulfilled by Swiss-model (<http://swissmodel.expasy.org/>). Phylogenetic trees constructed from the alignment were generated by the Neighbor-joining method using MEGA5.0 software. Reliability of trees obtained was assessed by bootstrapping, using 1000 bootstrap replications.

Quantification of AwCaM1 expression by real-time PCR

To determine the mRNA levels of AwCaM1 derived from hepatopancreas and other tissues, real-time quantitative PCR was underdone following the manufacture instruction of SYBR Premix Ex TaqTM (TaKaRa, China). Firstly, AwCaM1 primers as well as β -actin primers (Table 1) were designed based on isolated sequences of *A. woodiana*, respectively, used to isolated target genes in common PCR instrument, and only one band was detected in the PCR production by agarose gel electrophoresis. PCR products were sequenced and identified as the partial sequence of target genes. Subsequently, real-time PCR was fulfilled using an ABI 7500 Real-Time Detection System (Applied

Biosystems, USA). Based on constructed standard curve, expression levels of AwCaM1 were calculated by $2^{-\Delta\Delta CT}$. All data were given in terms of relative mRNA expression as means \pm SE.

Statistical analyses

All of the experimental data analyses were subjected to one-way analysis of variance (ANOVA) and $p < 0.05$ was considered statistically significant.

Results

Characterization of AwCaM1 cDNA

The complete cDNA sequence of AwCaM1 was obtained and deposited in GenBank under accession number KY996397, and comprised of 692 bp, including a 5' untranslated region (UTR) of 21 nucleotides, a 516 bp open reading frame (ORF) which was encoded 172 amino acids, and a long 3'-UTR of 155 nucleotides containing a stop codon (TAG), a putative polyadenylation consensus signal (AATAAA), and a poly (A) tail (Figure 1). The calculated molecular mass of deduced mature AwCaM1 was 19.22 kDa and had a theoretical isoelectric point of 4.07. AwCaM1 contained four putative Ca²⁺-binding EF-hand motifs which were respectively located at 34–63 aa, 71–99 aa, 108–136 aa and 144–172 aa (Figure 1). Comparing the variance of amino acid sequences, the conserved amino acid residues were highly found in AwCaM1 and CaM of others. Two crucial phosphorylation sites of the human CaM (Thr⁷⁹ and Ser⁸¹) were respectively identified in AwCaM1 (102 aa and 104 aa) (Figure 2). Notably, alignment result showed only three residues of Arg⁷⁵ and Ile⁸⁶ and Tyr¹⁰⁰ in human were respectively substituted by Lys, Leu and Phe in AwCaM1 (Figure 2).

Furthermore, predicted secondary structure of AwCaM1 protein contained seven alpha-helices and eight β -sheets (Figure 3A) that was very similar to CaM secondary structure of other species, especially to that of human. 3D structure of AwCaM1 showed a high-degree similarity with CaMs (Figure 3B).

Evolutionary relationship of AwCaM1

BLAST analysis revealed that amino acid sequence of AwCaM1 was close with other CaMs. The overall deduced amino acid sequence of AwCaM1 exhibited 96% to

	AGTGGTATCAACGCAGAGTAC	21
ATGGGGGAATCTTAACAGGTAGAAATTTTAAATTGTGAGCGCAAATCAAAGAACTA		81
M G G I L T G R N F K F V S G K S K K L		20
CAATCCGCGATGGCCGACCAGTTGACAGAAGAACAAATTGCCGAATTCAAGGAGGCATT		141
Q S A M A D Q L T E E Q I A E F K E A F		40
AGCCTGTTTGACAAGGACGGGGATGGAACCATCACTACCAAGGAACTGGGGACAGTGATG		201
S L F D K D G D G T I T T K E L G T V M		60
AGGTCCCTGGGACAAAATCCAACAGAGGCCGAATTCAGGATATGATTAAACGAAGTGGAT		261
R S L G Q N P T E A E L Q D M I N E V D		80
GCCGATGGTAATGGAACGATTGATTTCCCGGAATTCCTCACAATGATGGCAAAAAGATG		321
A D G N G T I D F P E F L T M M A K K M		100
AAGGATACAGATTGAGAAGAAGATTACGCGAGGCGTTTCGAGTCTTTGACAAAGACGGA		381
K D T D S E E E L R E A F R V F D K D G		120
AATGGCTTTATCAGTGCAGCAGAACTCAGACACGTGATGACAAATCTCGGGGAAAAGCTC		441
N G F I S A A E L R H V M T N L G E K L		140
ACAGACGAGGAGGTCGACGAGATGATCCGAGAAGCAGATATTGACGGAGATGGCCAAGTA		501
T D E E V D E M I R E A D I D G D G Q V		160
AATTATGAAGAATTTCGTGCAGATGATGTCGAGTAAATGAAAATAATAAGAGGATAAAGCT		561
N Y E E F V Q M M S S K *		172
GTGGATGGACATAACTAATGCAAATGTTTTTCACGATATTGTATTTTATACATTTTATT		621
TTTAAATTATTTAAATATAAATAAAATAAACTATCTGAAAGAAAAAAAAAAAAAAAAAAAA		681
AAAAAAAAAAAA		692

Figure 1: Nucleotide and deduced amino acid sequences of AwCaM1.

The start and stop codons are indicated with bold. Putative polyadenylation signal “AATAAA” is showed with wavy line. The four Ca^{2+} -binding domains are marked with box.

freshwater bivalve *Pinctada fucata*, 94% to insect *Daphnia magna*, 96% to *Drosophila melanogaster* and 95% with *Homo sapiens*. A molecular phylogenetic tree was generated to further analyze the evolutionary relationships between AwCaM1 and other CaMs sequences (Figure 4). In evidenced sequences of mollusk, AwCaM1 shared the higher relationship of evolution with clam of freshwater. Interestingly, the freshwater calms and seawater ones were not grouped in one cluster although they were belonged to same class (Figure 4). In addition, species were not orderly arranged according to evolutionary relationship, such as spider *Cupiennius salei*, holothuroidea *Apostichopus japonicas*, fish *Branchiostoma belcheri tsingtauense* located in one cluster as well as chordata *Ciona intestinalis*, camel *Camelus dromedaries*, *Homo sapiens*,

bird *Cariama cristata* distributed in one clade (Figure 4). Notably, few lower bootstrap values were observed between two classes (Figure 4).

Analysis of two premature termination codon mutations of AwCaM1

Two premature termination codon mutations of CaM from *A. woodiana* were isolated and named as AwCaM2 (GenBank accession number KY996398) and AwCaM3 (GenBank accession number KY996399), their full cDNA lengths were 610 bp and 546 bp, respectively. The AwCaM2 and AwCaM3 share similar sequence composition with AwCaM1 from 1st to 535th bp (Figure 5). In contrasted with

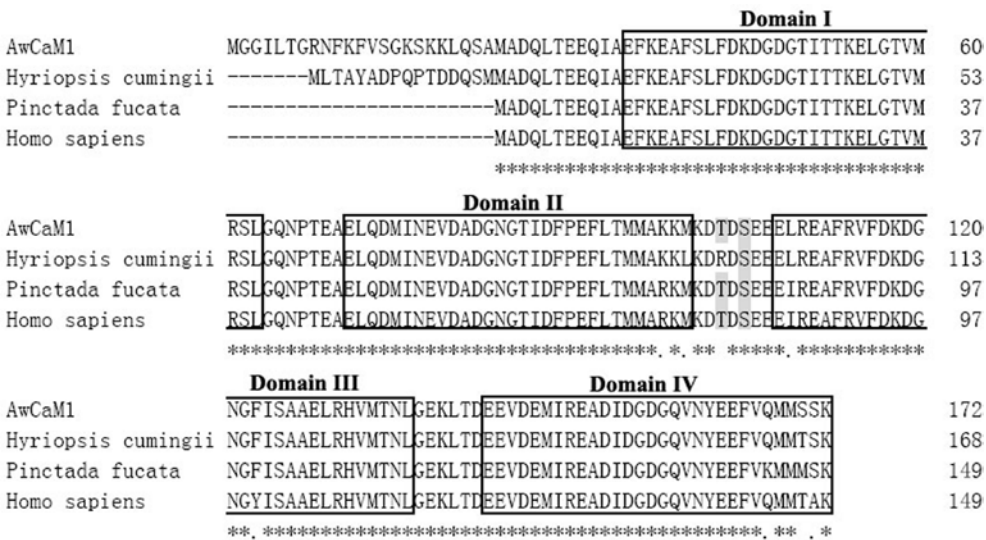


Figure 2: Multiple alignment of AwCaM1 with other CaMs. Two crucial phosphorylation sites of Thr and Ser are indicated with shadow. The four Ca²⁺-binding domains are marked with box.

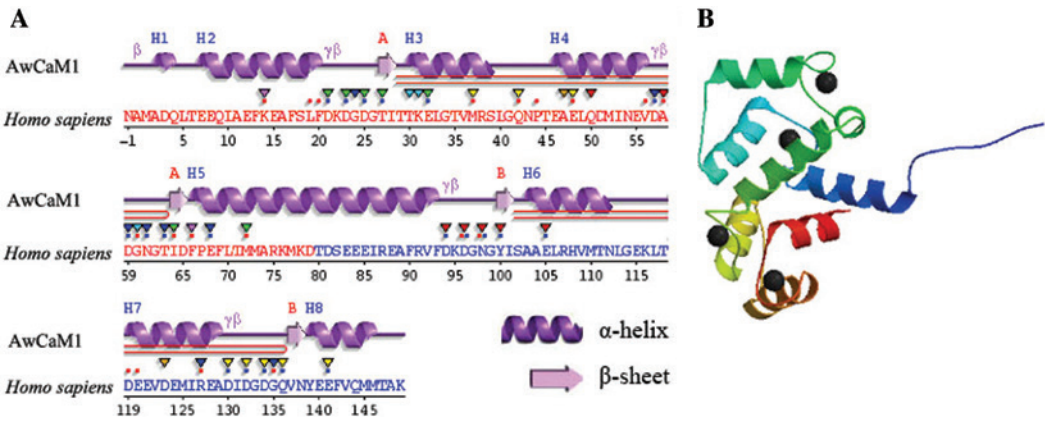


Figure 3: Predicted secondary and 3D structures of AwCaM1 deduced amino acids. (A) The secondary structure of AwCaM1. (B) The 3D structure of AwCaM1.

cDNA sequence of AwCaM1, AATAA signal sequence was missed in 3' UTR of AwCaM2, stop-code and AATAA signal sequences lacked in the AwCaM3 (Figure 5). Therefore, AwCaM2 and AwCaM3 were the individuals of premature termination codon mutations of CaM transcription.

Tissue distribution of AwCaM1

Quantitative real-time PCR was employed to investigate the distribution of AwCaM1 in different tissues. The constitutive expression levels of AwCaM1 were examined in different tissues including foot, mantle, adductor muscle, heart, hepatopancreas, hemocytes and gill, and showed different expression profiles (Figure 6). Higher expressions

of AwCaM1 were observed in mantle and gill, a moderate level in hepatopancreas, foot and heart, but a lower level in adductor muscle and hemocytes (Figure 6).

Ca²⁺ and Cd²⁺ effect on the siphoning behavior

No statistical difference of the siphoning behavior was observed between the control group and lower concentration Ca²⁺ treated groups (0.01, 0.02, 0.04 and 0.08 mg/L) (Figure 7). However, the filtration rate at 0.16 mg/L Ca²⁺ (24.84 ± 3.04 mL/animal/h) was significantly decreased compared with that of the control group (38.38 ± 3.12 mL/animal/h) (p = 0.0039) (Figure 7). In

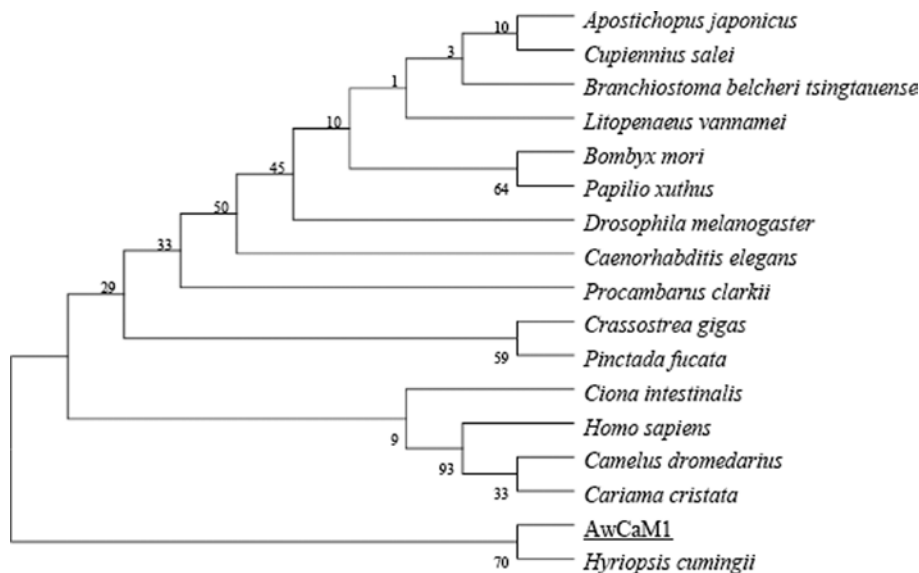


Figure 4: Phylogenetic relation of AwCaM1 from other organisms.

AwCaM1 is marked with underline. *Crassostrea gigas* (accession number XP_011436578.1), *Ciona intestinalis* (accession number NP_001027633.1), *Cuipeinnius salei* (accession number CFW94154.1), *Drosophila melanogaster* (accession number NP_523710.1), *Papilio xuthus* (accession number KPI95926.1), *Caenorhabditis elegans* (accession number NP_503386.1), *Procambarus clarkii* (accession number AC15835.1), *Camelus dromedarius* (accession number XP_010996006.1), *Cariama cristata* (accession number XP_009702107.1), *Pinctada fucata* (accession number JAS03530.1), *Litopenaeus vannamei* (accession number AEK21539.1), *Hyriopsis cumingii* (accession number ADT61781.1), *Apostichopus japonicus* (accession number AAY41437.1), *Bombyx mori* (accession number XP_012546645.1), *Homo sapiens* (accession number NP_001734.1), *Branchiostoma belcheri tsingtauense* (accession number ABM53481.1).

addition, administration different concentrations of Cd^{2+} could result in a decrease of filtration rate (Figure 7). Compared with that of control group, filtration rate of individual clam reduced more than 31.37% ($p=0.0106$), 56.04% ($p=0.0006$), 64.35% ($p=0.0003$) and 87.38% ($p=0.0001$) in the 2, 4, 8 and 16 mg/L of Cd^{2+} treated group, respectively.

Temporal expressions of AwCaM1 in hepatopancreas exposed to Ca^{2+} and Cd^{2+}

Temporal expressions of AwCaM1 mRNA in hepatopancreas were significantly affected by Ca^{2+} and Cd^{2+} challenge using RT-qPCR with β -actin as internal control (Figure 8). In the Ca^{2+} treated groups (0.01, 0.02, 0.04 and 0.08 mg/L), profiles of AwCaM1 expression showed a time and dose dependent pattern with respect of that of control group during experiment observed (Figure 8A). Meanwhile, in the Ca^{2+} treated groups (0.08 and 0.16 mg/L), AwCaM1 expression increased more than 56.15% ($p=0.0003$) from 6 h to 72 h (Figure 8A). In the Cd^{2+} treated groups (1, 2 and 4 mg/L), up-regulation of AwCaM1 expression showed a timed and dose dependent patten compared with that of control group (Figure 8B). In the Cd^{2+} treated groups (8 and 16 mg/L), AwCaM1 mRNA levels increased more 65.04% ($p=0.0001$) from 6 h to 72 h (Figure 8B).

Temporal expressions of AwCaM1 in gill exposed to Ca^{2+} and Cd^{2+}

In gill, treatment of different concentrations of Ca^{2+} caused a significant induction of AwCaM1 expression. Up-regulation of AwCaM1 expressions characterized with a timed and dose dependent patten was observed in the Ca^{2+} treated groups (0.01, 0.02, 0.04 and 0.08 mg/L) from 6 h to 72 h (Figure 9A). Among of all the Ca^{2+} treated groups, AwCaM1 expression increased more than 79.41% ($p=0.0001$) compared with that of control group (Figure 9A). Like mode of Ca^{2+} treatment, administration of Cd^{2+} could result in a significant up-regulation of AwCaM1 expression. In all the Cd^{2+} treated groups, AwCaM1 expression increased more than 88.23% ($p=0.0001$) in contrasted with that of control group (Figure 9B).

Temporal expressions of AwCaM1 in mantle exposed to Ca^{2+} and Cd^{2+}

In the mantle, up-regulation of AwCaM1 expression with a time and dose dependent pattern was observed in the Ca^{2+} treated groups (0.01, 0.02, 0.04 and 0.08 mg/L) during experiment observed (Figure 10A). With Ca^{2+} treatment at a concentration of 0.16 mg/L, AwCaM1 expression increased

AwCaM1.nr	AGTGGTATCAACGCAGAGTACATGGGGGGAATCTTAACAGGTAGAAATTTTAAATTTGTG	60
AwCaM2.nr	AGTGGTATCAACGCAGAGTACATGGGGGGAATCTTAACAGGTAGAAATTTTAAATTTGTG	60
AwCaM3.nr	AGTGGTATCAACGCAGAGTACATGGGGGGAATCTTAACAGGTAGAAATTTTAAATTTGTG	60
Consensus	ag t g g t a t c a a c g c a g a g t a c a t g g g g g g a a t c t t a a c a g g t a g a a a t t t t a a a t t t g t g	
AwCaM1.nr	AGCGGCAAAATCAAAGAACTACAATCCGCGATGGCCGACCAGTTGACAGAAGAACAATTT	120
AwCaM2.nr	AGCGGCAAAATCAAAGAACTACAATCCGCGATGGCCGACCAGTTGACAGAAGAACAATTT	120
AwCaM3.nr	AGCGGCAAAATCAAAGAACTACAATCCGCGATGGCCGACCAGTTGACAGAAGAACAATTT	120
Consensus	a g c g g c a a a t c a a a g a a a c t a c a a t c c g c g a t g g c c g a c c a g t t g a c a g a a g a a c a a t t t	
AwCaM1.nr	GCCGAATTCAGGAGGCATTACAGCCTGTTTGACAAGGACGGGGATGGAACCATCACTACC	180
AwCaM2.nr	GCCGAATTCAGGAGGCATTACAGCCTGTTTGACAAGGACGGGGATGGAACCATCACTACC	180
AwCaM3.nr	GCCGAATTCAGGAGGCATTACAGCCTGTTTGACAAGGACGGGGATGGAACCATCACTACC	180
Consensus	g c c g a a t t c a g g a g g c a t t a c a g c c t g t t t g a c a a g g a c g g g g a t g g a a c c a t c a c t a c c	
AwCaM1.nr	AAGGAACTGGGGACAGTGATGAGGTCCCTGGGACAAAATCCAACAGAGGCCGAACCTTCAG	240
AwCaM2.nr	AAGGAACTGGGGACAGTGATGAGGTCCCTGGGACAAAATCCAACAGAGGCCGAACCTTCAG	240
AwCaM3.nr	AAGGAACTGGGGACAGTGATGAGGTCCCTGGGACAAAATCCAACAGAGGCCGAACCTTCAG	240
Consensus	a a g g a a c t g g g g a c a g t g a t g a g g t c c c t g g g a c a a a a t c c a a c a g a g g c c g a a c t t c a g	
AwCaM1.nr	GATATGATTAAACGAAGTGGATGCCGATGGTAATGGAACGATTGATTTCCCGGAATTCCTC	300
AwCaM2.nr	GATATGATTAAACGAAGTGGATGCCGATGGTAATGGAACGATTGATTTCCCGGAATTCCTC	300
AwCaM3.nr	GATATGATTAAACGAAGTGGATGCCGATGGTAATGGAACGATTGATTTCCCGGAATTCCTC	300
Consensus	g a t a t g a t t a a c g a a g t g g a t g c c g a t g g t a a t g g a a c g a t t g a t t t c c c g g a a t t c c t c	
AwCaM1.nr	ACAATGATGGCAAAAAGATGAAGGATACAGATTCAGAAGAAGAATTACGCGAGGCGTTT	360
AwCaM2.nr	ACAATGATGGCAAAAAGATGAAGGATACAGATTCAGAAGAAGAATTACGCGAGGCGTTT	360
AwCaM3.nr	ACAATGATGGCAAAAAGATGAAGGATACAGATTCAGAAGAAGAATTACGCGAGGCGTTT	360
Consensus	a c a a t g a t g g c a a a a a g a t g a a g g a t a c a g a t t c a g a a g a a g a a t t a c g c g a g g c g t t t	
AwCaM1.nr	CGAGTCTTTGACAAAGACGGAAATGGCTTTATCAGTGCAGCAGAACTCAGACACGTGATG	420
AwCaM2.nr	CGAGTCTTTGACAAAGACGGAAATGGCTTTATCAGTGCAGCAGAACTCAGACACGTGATG	420
AwCaM3.nr	CGAGTCTTTGACAAAGACGGAAATGGCTTTATCAGTGCAGCAGAACTCAGACACGTGATG	420
Consensus	c g a g t c t t t g a c a a a g a c g g a a a t g g c t t t a t c a g t g c a g c a g a a c t c a g a c a c g t g a t g	
AwCaM1.nr	ACAAATCTCGGGGAAAAGCTCACAGACGAGGAGGTCGACGAGATGATCCGAGAAGCAGAT	480
AwCaM2.nr	ACAAATCTCGGGGAAAAGCTCACAGACGAGGAGGTCGACGAGATGATCCGAGAAGCAGAT	480
AwCaM3.nr	ACAAATCTCGGGGAAAAGCTCACAGACGAGGAGGTCGACGAGATGATCCGAGAAGCAGAT	480
Consensus	a c a a a t c t c g g g g a a a a g c t c a c a g a c g a g g a g g t c g a c g a g a t g a t c c g a g a a g c a g a t	
AwCaM1.nr	ATTGACGGAGATGGCCAAGTAAATTTATGAAGAATTCGTGCAGATGATGTCGACTAAATGA	540
AwCaM2.nr	ATTGACGGAGATGGCCAAGTAAATTTATGAAGAATTCGTGCAGATGATGTCGACTAAATGA	540
AwCaM3.nr	ATTGACGGAGATGGCCAAGTAAATTTATGAAGAATTCGTGCAGATGATGTCGACTAAATGA	540
Consensus	a t t g a c g g a g a t g g c c a a g t a a a t t a t g a a g a a t t c g t g c a g a t g a t g t c g a g t a a a t g a	
AwCaM1.nr	AAATTAATAGAGGATAAAGCTGTGGATGGACATAACTAATGCAAAATGTTTTTCACGATAT	600
AwCaM2.nr	AAATTAATAGAGGATAAAGCTGTGGATGGACATAACTAATGCAAAATGTTTTTCACGATAT	600
AwCaM3.nr	AAAAAA.....	546
Consensus	a a a t a a t a a g a g g a t a a a g c t g t g g a t g g a c a t a a c t a a t g c a a a a a a a a a a a a a a a a	
AwCaM1.nr	TGTATTTTATACATTTTATTTTAAATTATTTAAATATAAATAAAATAAACTATCTGA	660
AwCaM2.nr	AAAAA.....	610
AwCaM3.nr	546
Consensus	a a	
AwCaM1.nr	AAGAAAAAAAAAAAAAAAAAAAAAAAAAAAAA	692
AwCaM2.nr	610
AwCaM3.nr	546
Consensus		

Figure 5: Alignment of nucleotide sequences of AwCaM1, AwCaM2 and AwCaM3.

Stop codons (TGA) are indicated with green box. Putative polyadenylation signal "AATAAA" is showed with red underline.

more than 1.69 times ($p=0.0001$) from 6 h to 72 h compared with that of control group (Figure 10A). In the Cd^{2+} treated groups (1, 2 and 4 mg/L), up-regulation of AwCaM1 expression showed a timed and dose dependent pattern. In the Cd^{2+} treated groups (8 and 16 mg/L), AwCaM1 mRNA levels increased more 1.65 times ($p=0.0001$) from 6 h to 72 h in contrasted with that of control group (Figure 10B).

Discussion

CaM is a pivotal calcium metabolism regulator and involved into the shell formation process of the pearl oyster. In current study, one complete cDNA sequence of CaM gene was isolated from freshwater bivalve *A. woodiana* and named AwCaM1, and its expression

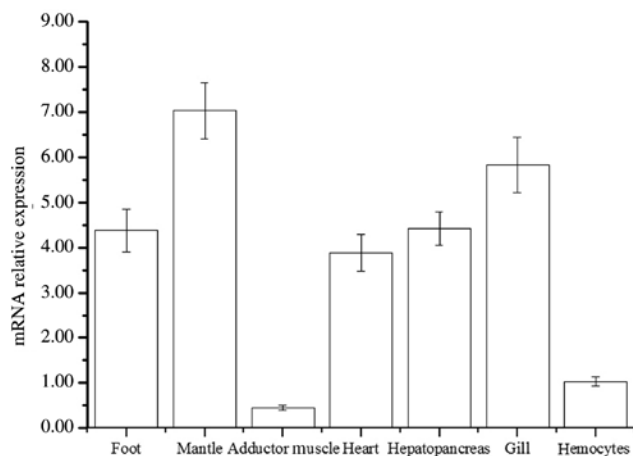


Figure 6: Real-time PCR analysis of AwCaM1 transcript from different tissues.
n = 3 Replicates.

was also examined in different tissues and different times.

The deduced primary amino acid sequence of AwCaM1 showed a high identity with the published CaMs of a range of invertebrate and vertebrate species. With respect to difference of amino acid composition, only three amino acid residues were observed between AwCaM1 and human CaM. Meanwhile, the CaM genes from different vertebrate species encode the same CaM molecule with high identical amino acid sequences. In current study, AwCaM1 was also identified with that from crustacean *D. magna*, and insect *D. melanogaster*, which indicates that the CaM proteins are highly conserved during invertebrate evolution. Notably, residue substitution, an interesting phenomenon, was detected in the present study. Compared to the marine pearl oyster *P. fucata* CaM, there is a single-amino acid substitution at position 147 in which Met is occupied by the Thr in freshwater bivalve *Hyriopsis cumingii* and Ser in *A. woodiana*, respectively. The Met at this position in *P. fucata* is considered to be a characteristic residue of the oyster [18], but it is not found in these freshwater clams. What reasons of substitution between oyster and freshwater clams are needed be further elucidate. In addition, compared with the deduced protein sequences, an important phosphorylation site Tyr100 in the Ca^{2+} -binding ligand position of the third EF-hand motif of human Cam was substituted by Phe100 in AwCaM1. It has demonstrated that phosphorylation of Tyr100 in human works as important role of increase binding affinity for its target proteins [19]. The substitution of phosphorylation sites of 100 aa is likely associated with the regulation of AwCaM1 at the posttranscriptional level. On another hand, as a key binding site of EF-hand motif, event of substitution should result in a

conformational change of this protein that further effect its affinity for most of its target proteins and its ability to activate target proteins. To shed light of these phenomena is a very interesting work in the future.

CaM, a multifunctional Ca^{2+} binding protein, is involved in the regulation of numerous important physiological functions, including neural activity, gene expression, enzyme regulation and muscle contraction. CaM is highly conserved across different species, and comprised of four EF hands that generally form two structurally similar domains connected by a flexible central linker. Although CaMs of these species are highly conserved and share similar structure, phylogenetic result showed that few lower bootstrap values were observed in different clusters in these CaMs located. An obvious distance of phylogenetic relationship was also detected between freshwater calms and seawater ones in spite they all belong to one class. Meanwhile, different species derived from vertebrate and invertebrate were grouped into similar cluster. Based on mentioned above, it is suggested CaM is not a candidate for reflecting the phylogenetic relationship, but an important player for sustaining normal physiological function of animals.

In all the tissues, strong expression of AwCaM1 was observed in mantle, suggested that is associated with the shell formation. The original hypotheses indicate that CaM expression should be greater in epithelial tissues (such as the gill and mantle) and lesser in non-epithelial tissues (such as muscle) [20]. In mollusks, the mantle, especially the outer epithelium of the mantle, plays a key role in shell formation [21]. In current study, the AwCaM1 mRNA expression level was obvious higher in the mantle compared to the adductor muscle. Similar results are also reported from other animals. In addition, the higher expression level of AwCaM1 mRNA was observed in the gill that supports previous conclusion in which gill is considered as a key organ of calcium uptake and accumulation in the bivalve. It has demonstrated that the gill is a primary organ for calcium uptake from the water in bivalves. Particularly in the scallop, the gill is thought to play a regulatory role in the membrane Ca^{2+} -ATPase system or to act as a “calcium sink” [18].

In the current study, AwCaM2 and AwCaM3, two premature termination codon mutations of CaMs, were also isolated from *A. woodiana*, suggesting there is a complex mechanism involved into controlling AwCaM1 transcription. As to phenomena, studies of loss-of-function mutations pave an avenue to elucidate mechanism, it has gain great attention. Loss-of-function mutations are generally believed to be deleterious and have been discussed in the context of human medicine [22]. Now, genome wide

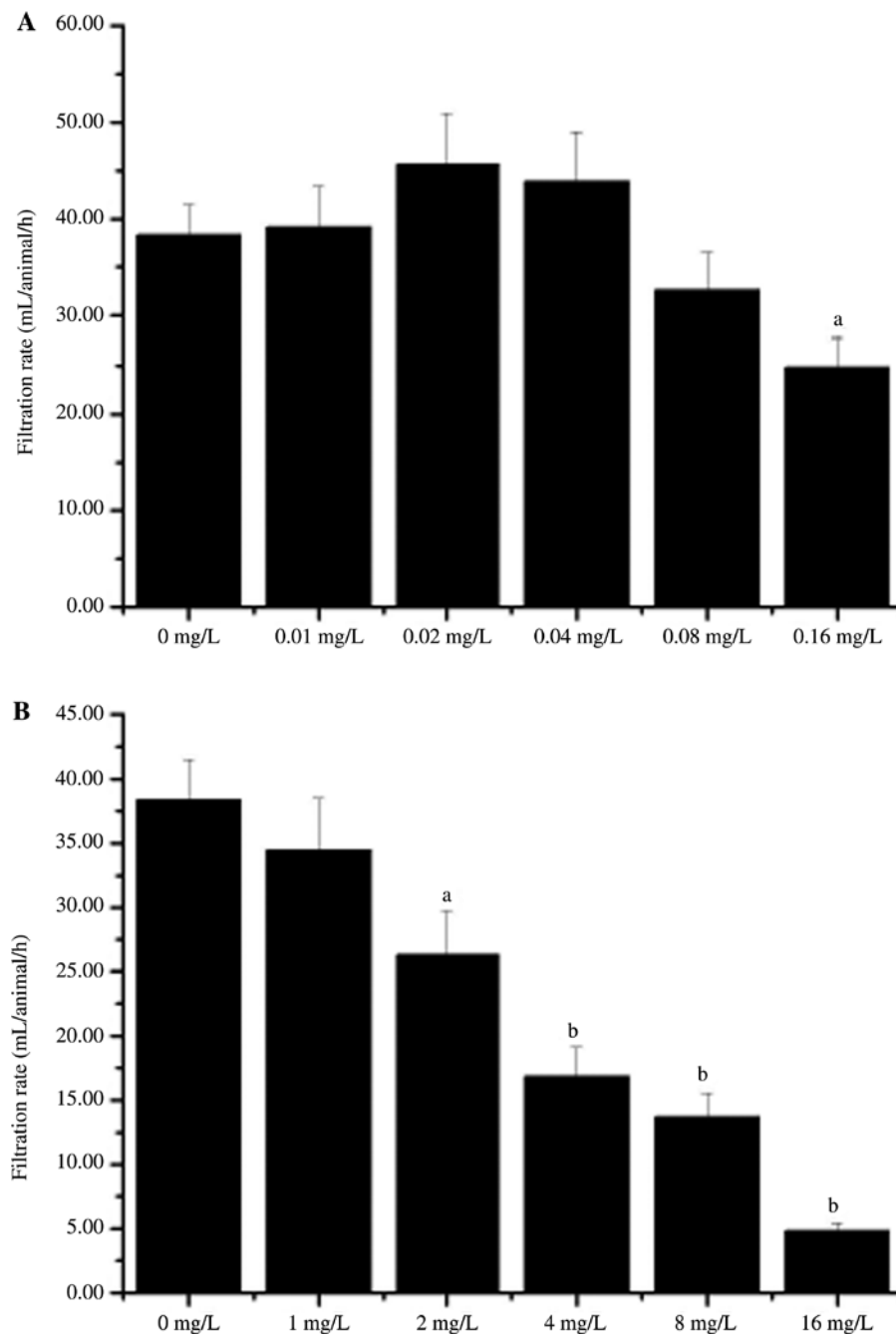


Figure 7: Filtration rate (mL/animal/h) of *Anodonta woodiana* exposed to Ca²⁺ and Cd²⁺ treated water. Average (n=5) filtration rate (mL/animal/h) of clams in Ca²⁺ and Cd²⁺ treated water containing a 1 mg/L neutral red solution (0–50 mg/L) following a 72-h exposure period to the concentrations indicated. The experiments were performed in triplicate and repeated three times with similar results. The bars display the mean \pm SE. A statistically significant difference between treatment group and control ($p < 0.05$) is indicated by differences in the letters above the bars. ^a $p < 0.05$, ^b $p < 0.01$ vs. control group at the treated group.

surveys in human and fly populations reveal an unexpected prevalence of loss-of-function mutations with hundreds or thousands of genes harboring deletions and/or premature termination codon mutations [23]. These genes are narrowly transcribed and encode high numbers of paralogs. But, gene expression in eukaryotes

is a compartmentalized process consisting of several different, yet connected steps. In the process, importance of gene expression for living cells and organisms is exemplified by the existence of diverse molecular mechanisms that detect errors and thereby ensure the accuracy of gene expression. A well-known quality control process, referred

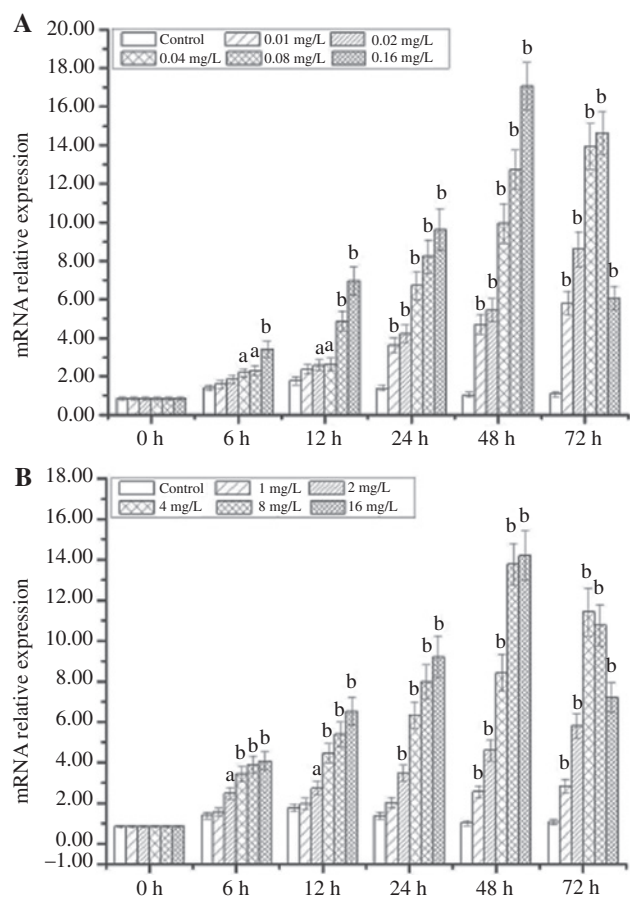


Figure 8: Temporal expressions of AwCaM1 in hepatopancreas after Ca^{2+} and Cd^{2+} challenge as measured by quantitative real-time PCR. (A) Effect of Ca^{2+} on AwCaM1 expression in hepatopancreas. (B) Effect of Cd^{2+} on AwCaM1 expression in hepatopancreas. Bars represented means \pm SE; $n=3$ /each group/each time point. $^a p < 0.05$, $^b p < 0.01$ vs. control group at the same time.

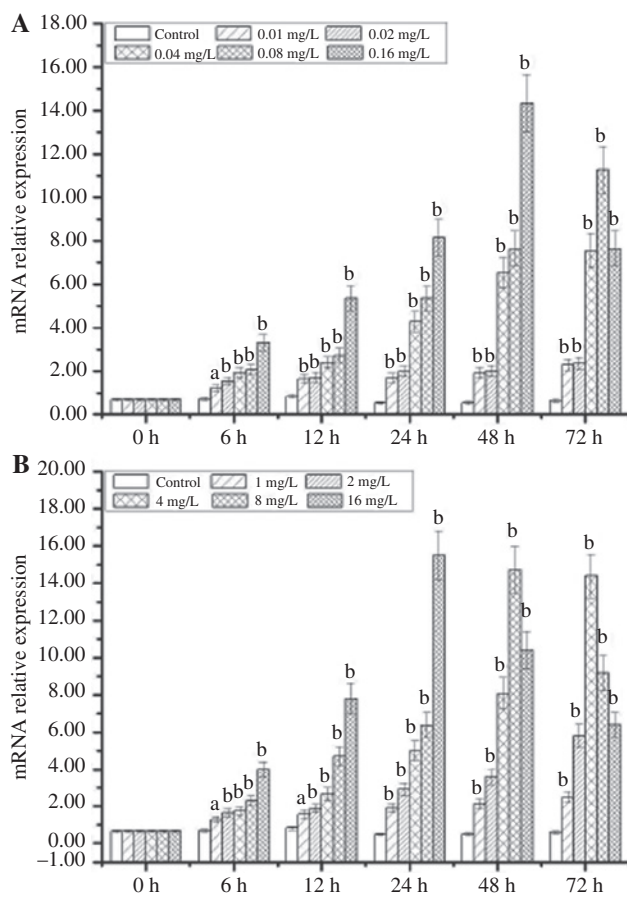


Figure 9: Temporal expressions of AwCaM1 in gill after Ca^{2+} and Cd^{2+} challenge as measured by quantitative real-time PCR. (A) Effect of Ca^{2+} on AwCaM1 expression in gill. (B) Effect of Cd^{2+} on AwCaM1 expression in gill. Bars represented means \pm SE; $n=3$ /each group/each time point. $^a p < 0.05$, $^b p < 0.01$ vs. control group at the same time.

to as nonsense-mediated mRNA decay or alternatively mRNA surveillance, limits the expression of mRNAs with premature termination codons and other aberrant termination events. So, in order to tolerate existence of these genes, a sophisticated mechanism should be involved in the regulated process of transcription [22, 23].

Filtration rates of Cd^{2+} treated groups were significant reduced compared with that of control group, suggesting that treatment of Cd^{2+} could result in an obvious injury on the health clams. Combination of siphoning behavior and valve movement has been utilized as indicators for continuous biomonitoring of water supplies and effluents [24]. Bivalve siphons play important roles in nutritional physiology, defense, and reproduction and are therefore a signal of general healthy or stress. Previous studies have demonstrated that bivalve siphoning can be influenced by metals or chlorpyrifos [17, 25]. Valves of the clams are always closed during exposure to 3.13 mg/L chlorpyrifos

treatments [26]. In addition, a reduction of siphoning activity as a response to chemical stress has also been observed that is associated with ammonia accumulation in the tissue, a reduction in oxygen exchange, and reduced feeding which could all have significant implications for survival, growth and reproduction of bivalves [25, 27]. Herein, we found that Cd^{2+} exposure decreased the filtration rates of clams, although no significant valve closure was observed. It is therefore reasonable to conclude that the decreased siphoning caused by Cd^{2+} exposure reflects an overall negative health impact and an indicator of chemical stress.

In the present study, treatment of different Ca^{2+} concentrations could result in a significant up-regulation of AwCaM1 expression in the hepatopancreas, gill and mantle, suggested that stimulating AwCaM1 transcription might help *A. woodiana* to maintain cytosolic Ca^{2+} homeostasis and gain compensatory Ca^{2+} absorption as well as

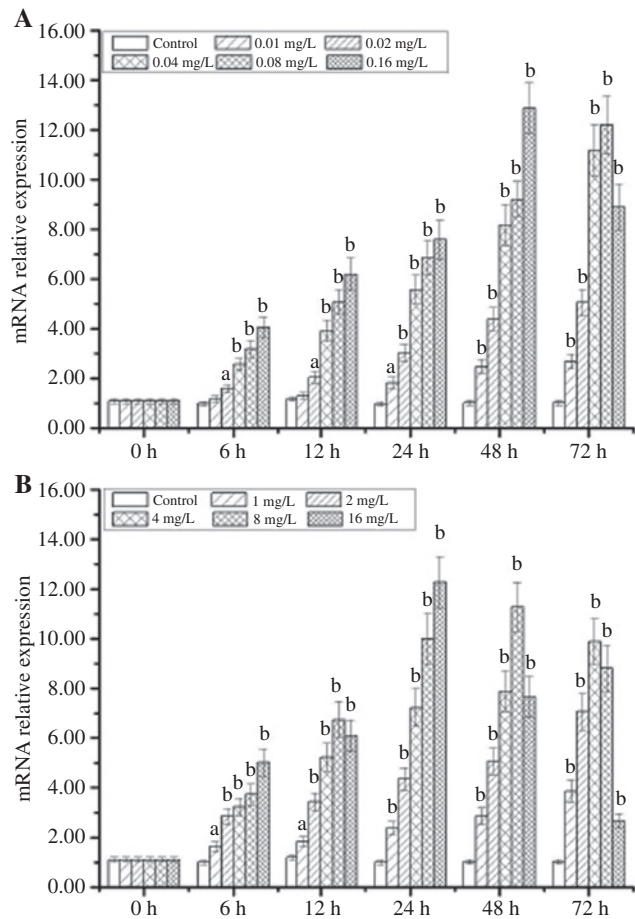


Figure 10: Temporal expressions of AwCaM1 in mantle after Ca^{2+} and Cd^{2+} challenge as measured by quantitative real-time PCR. (A) Effect of Ca^{2+} on AwCaM1 expression in mantle. (B) Effect of Cd^{2+} on AwCaM1 expression in mantle. Bars represented means \pm SE; $n=3$ /each group/each time point. ^a $p < 0.05$, ^b $p < 0.01$ vs. control group at the same time.

adapt to environmental stress. CaM plays a pivotal role in cellular Ca^{2+} homeostasis by activating Ca^{2+} -ATPase, which is the major transporter in Ca^{2+} fluxes [15, 28]. Up-regulation of AwCaM1 is contributed to increase Ca^{2+} absorption of cells. On another hand, in these tissues, expression of AwCaM1 was down-regulated at 72 h compared with that of 48 h in the Ca^{2+} treated group at a concentration of 0.16 mg/L. Significant up-regulation of AwCaM1 expression is also associated with coping environmental stress derived from Ca^{2+} treatment, especially in the higher concentration. Expression of CaMs of animals could be induced by environmental stressors, such as hypo-osmotic stress and pathogenic organism [21, 29]. Evidence has indicated that CaM is considered as one of the most important molecular biomarkers in teleost exposed to the chronic stressors [30]. Previous studies demonstrated that the cold adaptation in *Dissostichus mawsoni* is highly

related to CaM expression [31]. Given that CaM is an important subunit for several ion channels, the significant up-regulation of AwCaM1 expression likely function as dual role in the different concentrations of Ca^{2+} treatment.

In the hepatopancreas, gill and mantle, up-regulations of AwCaM1 with a time and dose dependent pattern were occurred in the Ca^{2+} treated groups at concentrations from 0.01 to 0.08 mg/L. In addition, filtration rates of Ca^{2+} treated groups showed a gradually up-regulation trend with respect of increase of treated concentrations between 0.01 and 0.04 mg/L. Combination of characterizations of AwCaM1 expression and filtration rate, we postulated, under 0.04 mg/L, administration of Ca^{2+} is contribute to increase absorption of Ca^{2+} and further maintain cytosolic Ca^{2+} homeostasis as well as boost shell formation of calms.

In the current study, treatment of Cd^{2+} at different concentrations could result in a significant up-regulation of AwCaM1 expression in the hepatopancreas, gills and mantle, suggested stimulation of AwCaM1 transcription is associated with Cd^{2+} toxicity. Due to their filtration activity, bivalves are exposed to numerous heavy metals and thus are subject to a considerable amount of oxidative damage [32]. It has found Cd^{2+} can induced oxidative DNA lesions in bivalves of freshwater and sea water. In the *Mytilus edulis*, low concentrations of Cd^{2+} enhance the genotoxicity of H_2O_2 and Cd^{2+} inhibits the DNA repair of 8-oxodG [33]. Further study shows that Cd^{2+} induced an increase of the DNA strand break levels and a low level of 8-hydroxy guanine DNA glycosidase-sensitive sites [34]. Undoubtedly, existence of Cd^{2+} can cause tremendous threat on cell survival. Notably, what is mechanism of Cd^{2+} entering into cells? Studies have indicated treatment of Cd^{2+} can cause break of Ca^{2+} homeostasis, and result in apoptosis of a variety of cells [35]. In the process, some Ca^{2+} related proteins are significantly up-regulated after Cd^{2+} exposure, such as neuronal calcium sensor, sarcoplasmic calcium-binding protein and CaM [35]. In addition, it was assumed that Ca^{2+} allow to be displaced by Cd^{2+} in some Ca^{2+} -binding proteins with respect of the biophysical similarities of Cd^{2+} and Ca^{2+} that disrupt Ca-mediated signaling pathways. Notably, research indicates Cd^{2+} exposure can lead to a transient rise in intracellular Ca^{2+} ions in several cell types, especially in osteoblasts [12]. Osteoblasts can uptake Cd^{2+} ions via membrane-bound transporters, such as transient receptor potential channels [36]. Consequently, it is possible that a combination of increased intracellular Cd^{2+} and Ca^{2+} ions can bind CaM leading to activation or inhibition of Ca^{2+} /calmodulin dependent kinase (CAMK) pathways. Other studies specifically implicate the CAMKII pathway as being activated by

Cd^{2+} exposure that result in apoptosis in cultured mesangial and neuronal cells [37]. However, the roles of the other two pathways, CaM-dependent PDE and CAMKK, in Cd^{2+} toxicity are under-investigated. Taken together, these studies provide evidence in support of the current research. Therefore, up-regulation of AwCaM1 is related with accumulation of Cd^{2+} that should lead to a risk of cell damage.

Notably, the AwCaM1 expressions of hepatopancreas, gill and mantle showed a dose- and time-dependent manner in lower concentration of Cd^{2+} treated groups. However, AwCaM1 expression showed a biphasic profile in the 8 and 16 mg/L of Cd^{2+} treated groups characterized by up-regulation matter in the early stage and down-regulation trend in the latter stage. This pattern of AwCaM1 is associated with persistent accumulation of reactive oxygen species (ROS) derived from Cd^{2+} injury. With elongation of Cd^{2+} treated time, ROS should increasingly be produced and accumulated in the cells. Levels of abruptly increased ROS is exceed the eliminating ability of cells that cause redox imbalance possibly via a shift between oxidants and antioxidants in favor of oxidants, and result in chronic inflammation, apoptosis of immune cells, etc. [38]. In the condition, if animals cannot produce new cells to compensate for death ones, number of living cells should be gradually decreased. Following, expressions of AwCaM1 are also decline alone treated time. Thus, a biphasic phenomenon was detected in higher concentration groups of Cd^{2+} .

In conclusion, one complete cDNA sequence and two premature termination codon mutations of CaMs (AwCaM1, AwCaM2 and AwCaM3) were cloned and characterized from the freshwater mussel *A. woodiana*. With respect of complex process from binding CaM to activation, effect of Ca^{2+} and Cd^{2+} on the freshwater bivalve *A. woodiana* is an sophisticated event. Use of AwCaM1 expression is contributed to provide insight into the important landscape of change at the molecular level derived from Ca^{2+} and Cd^{2+} treatment. This work is helpful to elucidate the potential mechanism of Cd^{2+} toxicity and provide a key regulator of Cd^{2+} toxicity in freshwater clam *A. woodiana*. The continuous functional investigation of proteins of network into Ca^{2+} involved could eventually solve the key targets of Cd^{2+} toxicity. Meanwhile, government should concern heavy metals diffusion and take measures to mitigate extensive negative impacts on freshwater organisms and conserve aquatic organism biodiversity. Notably, the present work is only the laboratory results. So, great efforts are required to explore the application of *A. woodiana* in the environmental engineering and environmental monitoring.

Acknowledgment: This research was funded by the National Natural Science Foundation of Henan (No. 18A330004, PXY-BSQD-2018009, 2015GGJS-286, 17A180010) and China Postdoctoral Science Foundation Funded Project (2016M590143).

References

1. Akphekhai LI, Oribhabor BJ. Nematodes relevance in soil quality management and their significance as biomarkers in aquatic substrates: review. *Recent Pat Biotechnol* 2016;10:228–34.
2. Tiling K, Proffitt CE. Effects of *Lyngbya majuscula* blooms on the seagrass *Halodule wrightii* and resident invertebrates. *Harmful Algae* 2017;62:104–12.
3. Le TT, Zimmermann S, Sures B. How does the metallothionein induction in bivalves meet the criteria for biomarkers of metal exposure? *Environ Pollut* 2016;212:257–68.
4. Suárez-Ulloa V, Fernández-Tajes J, Manfrin C, Gerdol M, Venier P, Eirín-López JM. Bivalve omics: state of the art and potential applications for the biomonitoring of harmful marine compounds. *Mar Drugs* 2013;11:4370–89.
5. Zhang X, Liu Z, Jeppesen E, Taylor WD. Effects of deposit-feeding tubificid worms and filter-feeding bivalves on benthic-pelagic coupling: implications for the restoration of eutrophic shallow lakes. *Water Res* 2014;50:135–46.
6. Chen J, Xie P. Seasonal dynamics of the hepatotoxic microcystins in various organs of four freshwater bivalves from the large eutrophic lake Taihu of subtropical China and the risk to human consumption. *Environ Toxicol* 2005;20:572–84.
7. Isani G, Andreani G, Cocchioni F, Fedeli D, Carpené E, Falcioni G. Cadmium accumulation and biochemical responses in *Sparus aurata* following sub-lethal Cd exposure. *Ecotoxicol Environ Saf* 2009;72:224–30.
8. Shi W, Zhao X, Han Y, Che Z, Chai X, Liu G. Ocean acidification increases cadmium accumulation in marine bivalves: a potential threat to seafood safety. *Sci Rep* 2016;6:20197.
9. Means AR, Dedman JR. Calmodulin – an intracellular calcium receptor. *Nature* 1980;285:73–7.
10. Zayzafoon M, Fulzele K, McDonald JM. Calmodulin and calmodulin-dependent kinase II α regulate osteoblast differentiation by controlling c-fos expression. *J Biol Chem* 2005;280:7049–59.
11. Shirran SL, Barran PE. The use of ESI-MS to probe the binding of divalent cations to calmodulin. *J Am Soc Mass Spectrom* 2009;20:1159–71.
12. Liu W, Zhao H, Wang Y, Jiang C, Xia P, Gu J, et al. Calcium-calmodulin signaling elicits mitochondrial dysfunction and the release of cytochrome c during cadmium-induced apoptosis in primary osteoblasts. *Toxicol Lett* 2014;224:1–6.
13. Chen S, Xu Y, Xu B, Guo M, Zhang Z, Liu L, et al. CaMKII is involved in cadmium activation of MAPK and mTOR pathways leading to neuronal cell death. *J Neurochem* 2011;119:1108–18.
14. Booth A, Zou E. Impact of molt-disrupting BDE-47 on epidermal ecdysteroid signaling in the blue crab, *Callinectes sapidus*, in vitro. *Aquat Toxicol* 2016;177:373–9.
15. Liu H, Chen X, Su Y, Kang JJ, Qiu X, Shimasaki Y, et al. Effects of calcium and magnesium ions on acute copper toxicity to

- Glochidia and early juveniles of the Chinese pond mussel *Anodonta woodiana*. *Bull Environ Contam Toxicol* 2016;97:504–9.
16. Evariste L, Rioult D, Brousseau P, Geffard A, David E, Auffret M, et al. Differential sensitivity to cadmium of immunomarkers measured in hemocyte subpopulations of zebra mussel *Dreissena polymorpha*. *Ecotoxicol Environ Saf* 2017;137:78–85.
 17. Cooper NL, Bidwell JR. Cholinesterase inhibition and impacts on behavior of the Asian clam, *Corbicula fluminea*, after exposure to an organophosphate insecticide. *Aquat Toxicol* 2006;76:258–67.
 18. Li S, Xie L, Ma Z, Zhang R. cDNA cloning and characterization of a novel calmodulin-like protein from pearl oyster *Pinctada fucata*. *FEBS J* 2005;272:4899–910.
 19. Corti C, Leclerc LE, Quadroni M, Schmid H, Durussel I, Cox J, et al. Tyrosine phosphorylation modulates the interaction of calmodulin with its target proteins. *Eur J Biochem* 1999;262:790–802.
 20. Tang M, Shi A. Studies of environmental calcium concentration effect on the calcium metabolism of the mantle and pearl sac of the freshwater pearl mussel. *J Sichuan Univ* 2000;37:741–7.
 21. Ren G, Hu X, Tang J, Wang Y. Characterization of cDNAs for calmodulin and calmodulin-like protein in the freshwater mussel *Hyriopsis cumingii*: differential expression in response to environmental Ca(2+) and calcium binding of recombinant proteins. *Comp Biochem Physiol B Biochem Mol Biol* 2013;165:165–71.
 22. Hug N, Longman D, Cáceres JF. Mechanism and regulation of the nonsense-mediated decay pathway. *Nucleic Acids Res* 2016;44:1483–95.
 23. Kurosaki T, Maquat LE. Nonsense-mediated mRNA decay in humans at a glance. *J Cell Sci* 2016;129:461–7.
 24. Chen WY, Jou LJ, Chen SH, Liao CM. A real-time biomonitoring system to detect arsenic toxicity by valve movement in freshwater clam *Corbicula fluminea*. *Ecotoxicology* 2012;21:1177–87.
 25. Moulton CA, Fleming WJ, Purnell CE. Effects of two cholinesterase-inhibiting pesticides on freshwater mussels. *Environ Toxicol Chem* 1996;15:131–7.
 26. Milam CD, Farris JL. Risk identification associated with iron-dominated mine discharges and their effect upon freshwater bivalves. *Environ Toxicol Chem* 1998;17:1611–9.
 27. Chen H, Zha J, Liang X, Li J, Wang Z. Effects of the human antiepileptic drug carbamazepine on the behavior, biomarkers, and heat shock proteins in the Asian clam *Corbicula fluminea*. *Aquat Toxicol* 2014;155:1–8.
 28. Snedden WA, Fromm H. Calmodulin as a versatile calcium signal transducer in plants. *New Phytol* 2001;151:35–66.
 29. Ji PF, Yao CL, Wang ZY. Two types of calmodulin play different roles in Pacific white shrimp (*Litopenaeus vannamei*) defenses against *Vibrio parahaemolyticus* and WSSV infection. *Fish Shellfish Immunol* 2011;31:260–8.
 30. Alves RN, Cordeiro O, Silva TS, Richard N, de Vareilles M, Marino G, et al. Metabolic molecular indicators of chronic stress in gilt-head seabream (*Sparus aurata*) using comparative proteomics. *Aquaculture* 2010;299:57–66.
 31. Chen Z, Cheng CH, Zhang J, Cao L, Chen L, Zhou L, et al. Transcriptomic and genomic evolution under constant cold in Antarctic notothenioid fish. *Proc Natl Acad Sci USA* 2008;105:12944–9.
 32. Emmanouil C, Sheehan TM, Chipman JK. Macromolecule oxidation and DNA repair in mussel (*Mytilus edulis* L.) gill following exposure to Cd and Cr(VI). *Aquat Toxicol* 2007;82:27–35.
 33. Pruski AM, Dixon DR. Effects of cadmium on nuclear integrity and DNA repair efficiency in the gill cells of *Mytilus edulis* L. *Aquat Toxicol* 2002;57:127–37.
 34. Michel C, Vincent-Hubert F. DNA oxidation and DNA repair in gills of zebra mussels exposed to cadmium and benzo(a)pyrene. *Ecotoxicology* 2015;24:2009–16.
 35. Ha TT, Burwell ST, Goodwin ML, Noeker JA, Heggland SJ. Pleiotropic roles of Ca(2+)/calmodulin-dependent pathways in regulating cadmium-induced toxicity in human osteoblast-like cell lines. *Toxicol Lett* 2016;260:18–27.
 36. Lévesque M, Martineau C, Jumarie C, Moreau R. Characterization of cadmium uptake and cytotoxicity in human osteoblast-like MG-63 cells. *Toxicol Appl Pharmacol* 2008;231:308–17.
 37. Liu Y, Templeton DM. Cadmium activates CaMK-II and initiates CaMK-II-dependent apoptosis in mesangial cells. *FEBS Lett* 2007;581:1481–6.
 38. Putnam CD, Arvai AS, Bourne Y, Tainer JA. Active and inhibited human catalase structures: ligand and NADPH binding and catalytic mechanism. *J Mol Biol* 2000;296:295–309.